Fountain Journal of Natural and Applied Sciences 2024; 13(2): 92 - 104

DOI: 10.53704/fujnas.v13i2.637

A publication of College of Natural and Applied Sciences, Fountain University, Osogbo, Nigeria.
Journal homepage: www.fountainjournals.com
ISSN: 2354-337X(Online),2350-1863(Print)

Green Synthesis of Graphene/Zinc Oxide Nanocomposite for Optoelectronic Applications

[1] Gbadero, D. S., [1]Adedokun, K. A., [1]Ojo A. O., [2]Oyewole, O. J., [3]Adegboyega, O., [4]Adenigba V. O., [1,5]Awodele, M. K. and [1,5]*Adedokun, O.

[1]Department of Pure and Applied Physics, Ladoke Akintola University of Technology, Ogbomoso, Nigeria.
[2]Department of Physics and Astronomy, The University of Southern Mississippi, Hattiesburg, MS, USA
[3]Department of Physical Science Education, Emmanuel Alayande University of Education, Oyo, Nigeria.
[4]Department of Science Laboratory Technology, Ladoke Akintola University of Technology, Ogbomoso, Nigeria.
[5]Nanotechnology Research Group (NANO[+]), Ladoke Akintola University of Technology, Ogbomoso, Nigeria

Abstract

This research presents a green synthesis of high-quality graphene (G), zinc oxide (ZnO) and graphene/zinc oxide (G/ZnO) nanocomposites. Zinc Oxide nanoparticles (ZnO NPs) were synthesised using *Amarus Pinnantum* extracts, while graphene was derived from *Bryophyllum Pinnatum* shoot plant extracts. The integration of graphene into the ZnO matrix was investigated to enhance its structural, optical, and electrical properties, particularly electron mobility. The synthesised materials were characterised using UV-Vis spectroscopy, Fourier Transform Infrared (FTIR) spectroscopy, X-ray Diffraction (XRD), and Scanning Electron Microscopy (SEM) with Energy Dispersive X-ray Spectroscopy (EDS). UV-Vis spectra revealed characteristic absorption bands for graphene, ZnO, and G/ZnO. FTIR analysis confirmed the presence of functional groups associated with each material, including 593 cm^{-1} (Zn-O bending vibrations), 1088 and 1459 cm^{-1} (C-H Alkyl group bending vibrations), 1583 cm^{-1} (C=C Aromatic stretching vibration), and 3467 and 3777 cm^{-1} (O-H Hydroxyl group stretching vibration) in the G/ZnO nanocomposites. Scanning Electron Microscopy (SEM) images showed spherical zinc oxide (ZnO) nanoparticles, a rough, flake-like graphene structure, and a porous, aggregated morphology for the G/ZnO nanocomposite. EDS analysis verified the elemental composition of the materials. The electrical properties of the G/ZnO nanocomposite were significantly improved compared to pure graphene and ZnO nanoparticles. The composite exhibited a higher current (4.62 μA) and lower resistivity (405.56 Ω·m) at a specific voltage (0.60 V). This enhancement is attributed to the formation of a percolative network within the composite, which facilitates efficient charge transfer and improves electron mobility. These findings suggest that the G/ZnO nanocomposite holds promise for applications in optoelectronic devices.

Keywords Green Synthesis; Zinc Oxide; Graphene; Nanocomposite; Optoelectronic Application

Introduction

Renewable energy sources, such as solar, wind, and hydroelectric power, offer sustainable alternatives (Sun *et al*., 2020). Solar energy, in particular, presents attractive prospects due to its abundance and zero greenhouse gas emissions. It

* Corresponding Author: orcid.org/0000-0002-7947-8415
Email address: oadedokun@lautech.edu.ng

has various applications, including electricity generation, heating, and transportation (Farghali *et al*., 2023). One of the most promising applications of solar energy is in the field of optoelectronics, which are electronic devices that convert light into electrical energy or vice versa, for instance, solar cells and Light Emitting Diode (LED) (Djuriić *et al*., 2010; Machín & Márquez, 2024). Optoelectronic devices have various applications, including solar energy harvesting, optical communication systems, and display technologies (Chakraborty *et al*., 2024; Verduci *et al*., 2022). The production of optoelectronic devices requires materials with specific properties, such as high optical absorption, high carrier mobility, and high stability. Some of the commonly used materials for producing optoelectronic devices include silicon (Si), gallium arsenide (GaAs), and two-dimensional (2D) materials, such as graphene (Maalouf *et al*., 2023).

Two-dimensional (2D) semiconductors, such as Zinc Oxide (ZnO), have the advantages of a high concentration of free charge carriers, high carrier mobility, high conductivity, and high physical and chemical stability. These are critical for advancing the development of low-power and high-speed optoelectronic devices for practical applications (Hao *et al*., 2023). Zinc Oxide has attracted significant attention for various optoelectronic applications due to its non-toxicity, low cost, excellent chemical stability, wide range of radiation absorption, good electrical properties, and high electrochemical coupling coefficient. The physicochemical stability and ability to form in various morphologies and low-cost products attract increasing attention to ZnO-based applications. Zinc Oxide is a wide-band-gap transparent semiconductor with a band gap energy of ~3.37 eV with a large excitation binding energy of ~60 MeV. It also has high thermal and mechanical stability at room temperature, making it attractive for potential applications in electronics, laser technology, gas sensors, energy storage devices and optoelectronics (Wu *et al*., 2013; Sin Tee *et al*., 2016).

Graphene-based nanomaterials have attracted tremendous attention in the scientific community since their discovery in 2004. Graphene can act as an excellent electron acceptor due to its remarkable properties, such as excellent carrier mobility, superior thermal conductivity, good pore size distribution, high electrical conductivity, capacitive performance, and high surface area (2600 m^2 g^{-1}). Graphene is almost entirely transparent and can transmit up to 97.7% of light optically (Boutilier *et al*., 2014; O'Hern *et al*., 2014). Such exclusive properties of graphene have made it a promising candidate for incorporating ZnO-based nanomaterials to improve its optoelectronic devices significantly.

Furthermore, the formation of a nanocomposite with ZnO or other materials has recently been explored to improve its optoelectronic characteristics. The unique structural merits of composite materials, including electronic interactions, interfacial bonding, and synergistic effects, make them attractive for fabricating highly efficient optoelectronic devices. Recently, graphene-based materials decorated with metal/metal oxide nanoparticles have shown great promise for several technological applications (Gupta *et al*., 2015; Liu *et al*., 2015). The graphene/zinc oxide (G/ZnO) nanocomposite could enhance optoelectronic performance by facilitating the efficient migration of photo-induced electrons and suppressing electron-hole recombination during carrier transfer processes. Several routes for synthesising G/ZnO nanocomposites include sol gel, solvothermal, sonication, and microwave-assisted reaction methods (Nagaraj *et al*., 2020; Shahryari *et al*., 2021).

Existing synthesis methods to overcome the limitations of traditional methods, such as high costs, environmental harm, and toxicity, require a green synthesis approach. Green synthesis, also referred to as biological nanoparticle synthesis, involves the production of metal nanoparticles using bioactive agents such as plant materials, microbes, and various biowastes like vegetable and fruit peel waste, eggshells, agricultural waste, and algae (Kumar *et al*., 2021). Implementing reliable and sustainable green synthesis technologies is essential to avoid the creation of harmful byproducts.

This approach offers multiple benefits, such as simplicity, cost-effectiveness, time-efficiency, high-stability nanoparticles, non-toxic byproducts, and scalability for large-scale production (Malhotra & Alghuthaymi, 2022). This method is particularly advantageous for synthesising G/ZnO nanocomposites for optoelectronic applications. This study employs a green synthesis method to prepare G/ZnO nanocomposites to boost optical properties and efficiency. In the present study, G/ZnO nanocomposites were synthesised using a green synthesis approach. The ZnO nanoparticles and Graphene (G) were synthesised using the plant extract and plant shoot, respectively. The effects of Graphene on the morphology, structural, and optical properties of ZnO were investigated. Finally, a comparative study of the G/ZnO nanocomposites was also carried out.

Materials and Methods

Materials

The materials used were zinc acetate dihydrate {Zn $(CH_3COO)_2.2H_2O$} and sodium hydroxide (NaOH) procured from Sigma-Aldrich. Other reagents, such as ethanol (99.8 %) and de-ionised water, were purchased locally. Bryophyllum Pinnatum shoot plants and *Phyllanthus Amarus* leaves were harvested in the nearest farm garden in Ogbomoso.

Methods

Preparation of *Bryophyllum Pinnatum* Plant Shoot (Ewe Abamoda)

The *Bryophyllum Pinnatum* plant was sourced from a local farm in Ogbomoso, Oyo State, Nigeria. The plant was selected for biosynthesis due to its reducing properties, attributed to components like citric acid, ascorbic acid, flavonoids, reductases, and extracellular electron shuttles, all of which play a crucial role in nanoparticle biosynthesis. The *Bryophyllum Pinnatum* shoot plants were open-air-dried for several days and ground into a fine powder using a mortar and pestle. The sample was then placed in an electric furnace at 200 °C for 2 hours for carbonisation. Then, they store it for further use (Qu *et al*., 2013).

Preparation of Graphene using the plant shoot of *Bryophyllum Pinnatum*

Carbonised *Bryophyllum Pinnatum* shoot plants of 3 g were shaken (3000 rpm) in 250 ml of HNO_3 (2.50 mol L^{-1}) at 70 ºC for 300 min. The black precipitates in the mixture were separated using centrifugation (3000 rpm, 10 min). The residues derived from the filtrate were washed with ethanol 3 times to remove impurities and dried at 120 ºC for 2 h, and the products were collected (Qu *et al*., 2013).

Preparation of Plant Extract *Phyllanthus Amarus*

The fresh leaves of *Phyllanthus Amarus* were washed several times using deionized water to remove dirt particles. After washing, the leaves were left to sun dry and ground to a fine powder with a mortar. The fine powder leaves (about 5 g) were placed in a 250 mL beaker, mixed with 50 ml of deionised water and heated at 80 °C for 20 min. Then, the mixture was filtered into another beaker with Whatman no.1 filter paper, and the extract was formed at this stage (Rahman *et al*., 2022). The extract was then cooled down and stored in the refrigerator (4 °C) for utilisation in the synthesis of ZnO.

Preparation of Zinc Oxide Nanoparticles (ZnO NPs)

2.5 ml of plant extract was added to 25 ml of 0.5 M Zinc acetate dihydrate. The pH of the mixture was 6.13, 2 M NaOH was added dropwise to maintain pH at 8, then the mixture was then stirred and heated at 70 °C for 30 min for complete reduction and formation as shown in Figure 1. The resulting material was then collected via decantation, washed with distilled water to remove residuals, and oven-dried at 70 °C overnight to yield powdered ZnO NPs (Rahman *et al*., 2022). The synthesis steps are demonstrated in Figure 1. The dried sample was stored at room temperature in an airtight container for further characterization.

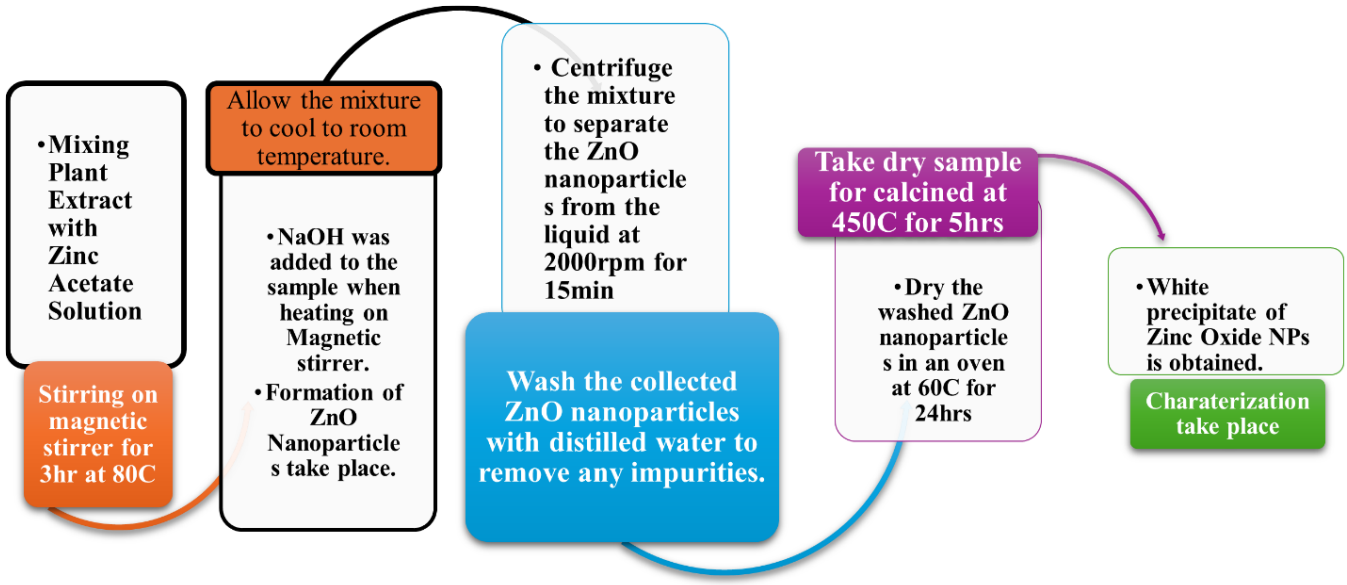

Figure 1: Schematic chart illustrating the green method of synthesis of ZnO NPs

Preparation of Graphene/Zinc Oxide Nanocomposites

G/ZnO NCs were prepared using the solution mixing method. The synthesised Graphene, ZnO NPs and ethanol were used as the starting materials for the synthesis of the G/ZnO NCs. First, 10 mg of the obtained G powder was dispersed in 10 mL of ethanol, and 200 mg of ZnO was dispersed in 20 mL of ethanol. These two solutions were then mixed homogeneously using an ultrasonic bath for one hour at room temperature and then transferred into a 100 mL treated at 180 °C for 24 h. The final products were centrifuged, washed with ethanol and distilled water, and dried at 60 °C for 12 h to obtain G/ZnO NCs (Kachere *et al*., 2021).

Film deposition using the doctor-blade method

The edge of 0.5 cm by 0.5 cm was made using adhesive tape on the conducting side of the Fluorine-doped Tin Oxide (FTO), such that FTO was first covered on two parallel edges with adhesive tape to control the areas of the films and to provide non-coated areas for electrical contact. The obtained pastes were applied to one of the free edges of the non-conducting glass substrates and distributed with a glass rod (spatula) sliding over the tape-covered edges. Also, the reference electrode was prepared without nanoparticles. They were left for 20 minutes to relax to reduce the surface irregularity and then dried for 45 minutes at 60 °C. Allow the film to dry for a sufficient amount of time (1 h) until it is completely dry. Perform additional post-processing steps, such as annealing or sintering, to improve the film's properties (Alamu *et al*., 2021; Shahryari *et al*., 2021). Optical characterisations were then carried out.

Characterisations

The resulting Graphene, ZnO NPs, and G/ZnO NCs were characterised using several characterisation techniques. The optical properties of the samples were studied through UV-visible absorbance using a double-beam UV-Vis-IR spectrophotometer (ASUV-6300PC) using an Xe lamp, as a function of wavelength in a wavelength range of 200-800 nm. The samples were analysed. X-ray diffraction (XRD) was conducted using the Rigaku D/Max-lllC diffractometer to identify structural phases of the samples. The analyses conducted with the diffractometer cover 2theta ranges from 10º to 90º, with a resolution of 0.001º 2theta. This allows for precise measurements of d-spacing between 0.1 and 2.0 nm. Fourier Transform Infrared Spectroscopy (FTIR) was performed using a Nicolet iS10 spectrometer in the mid-infrared

range. The experiment was carried out within the mid-infrared range, 400-4000 cm-1, at room temperature, with KBr as the diluting agent. Scanning Electron Microscopy (SEM) analysed the morphology and composition of the samples, capable of magnification up to 500,000x, about 250 times the magnification limit of the best light microscopes, with a resolution as fine as 1.0 nm. Operating within an accelerating voltage range of 0.1 kV to 30 kV, and equipped with multiple detectors for detailed nanoscale analysis, supported by Energy Dispersive X-ray (EDX) analysis (INCA 200, UK, at 20 keV) for elemental composition. Current-Voltage (I–V) characteristics of synthesised samples have been examined using a Four-Point Probes (4 PP) system equipped with Keithley 2400 source measuring unit,

Results and Discussion

Ultraviolet-visible (UV-Vis) Analysis of the samples

UV-vis spectroscopy was used to examine the optical absorption of graphene, zinc oxide nanoparticles, and a graphene/zinc oxide nanocomposite using a double-beam UV-Vis-IR spectrophotometer (ASUV-6300PC). The UV-vis absorption spectra of G, ZnO NPs and G/ZnO NCs are shown in Figure 2. The UV-Vis absorption spectra of G, ZnO NPs, and G/ZnO NCs are presented in Figures 2(a), 2(b), and 2(c), respectively.

The synthesised graphene exhibits absorption edges at 330 nm and 340 nm, attributed to n-π* electron transitions of the C=O bond (Huang *et al*., 2016). Zinc Oxide nanoparticles exhibit a sharp absorption edge at 295 nm, along with additional edges at 224 nm, 234 nm, and 242 nm, indicating the presence of ZnO nanoparticles (Arefi & Rezaei-Zarchi, 2012). The graphene/zinc oxide nanocomposites exhibit a broad absorption spectrum characterised by a sharp increase in absorbance around 300-400 nm, indicating strong absorption resulting from interactions between graphene and ZnO. This result aligns with previous reports, underscoring the significance of graphene in influencing the optical properties of ZnO (Kachere *et al*., 2021).

Fourier Transform Infrared Spectrometry (FTIR) Spectroscopy of the Synthesised Samples

The functional groups found on the surface of the nanoparticles were identified using an FTIR spectrometer. Figure 3 shows the spectra of G, ZnO nanoparticles (NPs), and G/ZnO nanocomposites (NCs). Table 1 lists the wavenumber values and absorption characteristics of all nanoparticles. FTIR spectroscopy was employed to analyse the molecular vibration frequencies of the synthesised G, ZnO nanoparticles, and G/ZnO nanocomposites. The FTIR spectra of G, ZnO NPs, and G/ZnO NCs are presented in Figures 3(a), 3(b), and 3(c), respectively.

The FTIR spectrum of graphene G exhibits absorption peaks at 3400 cm^{-1} (hydroxyl compound), 2354 cm^{-1} (C≡N stretching vibration of a nitrile group), 1618 cm^{-1} (C=C carbon-carbon Double Bond of an Alkene group), and 1029 cm^{-1} (C=O stretching vibration of an alcohol or ether). The Zinc Oxide nanoparticles (ZnO NPs) spectrum displays absorption peaks at 574 cm^{-1} (metal-oxygen vibration mode), 1032 cm^{-1} (C-O bond stretching vibration), and 1563 and 1495 cm^{-1} (N-H Amine, Nitrogen Hydrogen blending vibration, C=C Alkene carbon carbon stretching vibrations, respectively) (Jayarambabu *et al*., 2014; Hoseinpour *et al*., 2017; Khalil *et al*., 2020).

The G/ZnO NCs spectrum shows significant peaks at 593 cm^{-1} (Zn-O bending vibrations), 763 and 845 cm^{-1} (C-H bending vibrations), 1088 and 1459 cm^{-1} (C-H Alkyl group blending vibrations), 1583 cm^{-1} (C=C Aromatic stretching vibrations) and 3400, 3467 and 3777cm^{-1} (O-H Hydroxyl group stretching vibration). The FTIR analysis reveals the surface chemistry and interactions between graphene and zinc oxide nanoparticles, providing insights into the bonding characteristics and properties of the composite material (Payrazm *et al*., 2022).

X-ray Diffraction (XRD) of the samples

The XRD patterns of graphene, ZnO nanoparticles, and graphene/ZnO nanocomposite

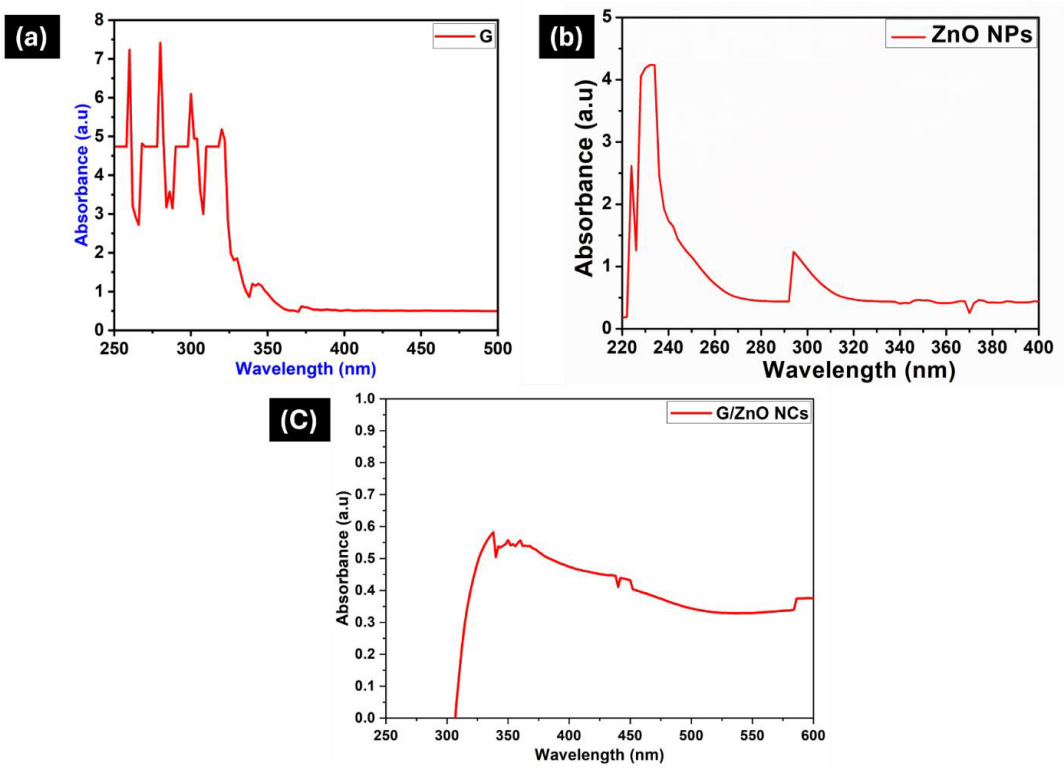

Figure 2: UV-Vis absorption spectra of synthesized (**a**) G (**b**) ZnO NPs and **(c)** G/ZnO NCs

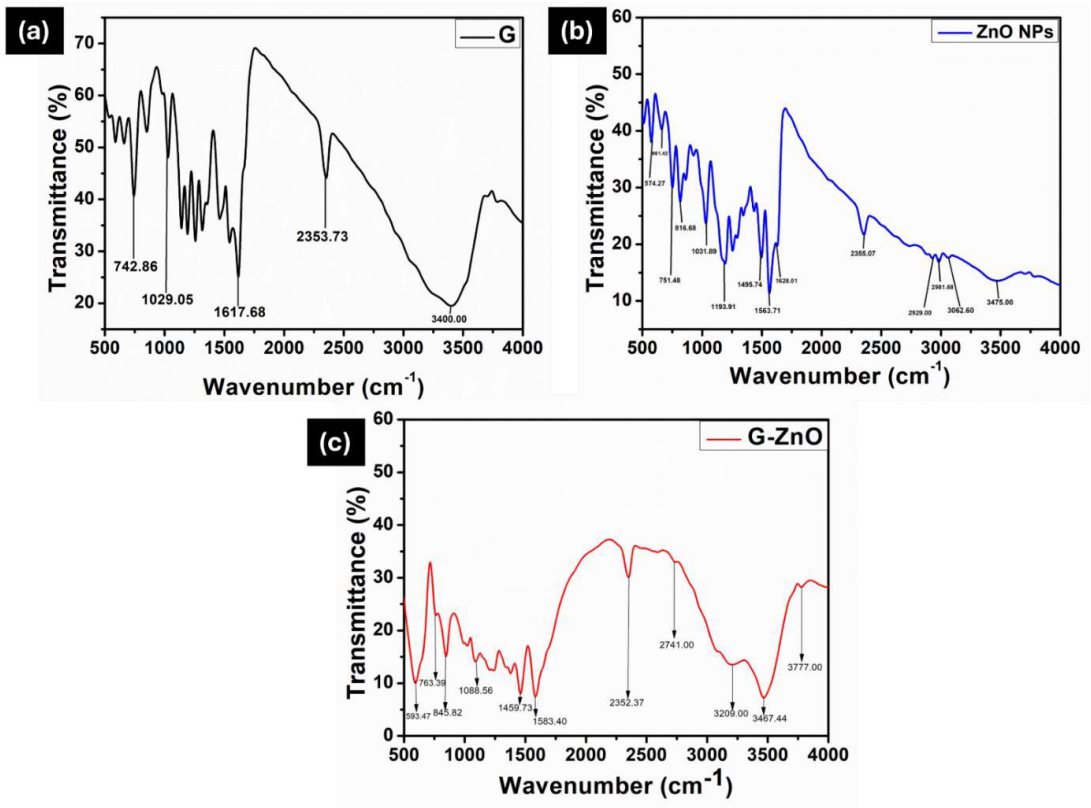

Figure 3: FTIR of synthesized (**a**) G, (**b**) ZnO NPs and **(c)** G/ZnO NCs

Table 1: The FTIR absorption value of the G, ZnO NPs, and G/ZnO NCs

Wave number (cm^{-1})	G	ZnO NPs	G/ZnO NCs	Functional group
3630-3200	3400	3475	3467	O-H stretch
3000-2850		3062	3209	C-H stretch
1680-1580	1617	1628	1580	C=C stretch
1400-1500		1495	1483	C-C stretch
1300-1000	1029	1031	1088	C-O stretch
900-650	742	751	845	C-H blend

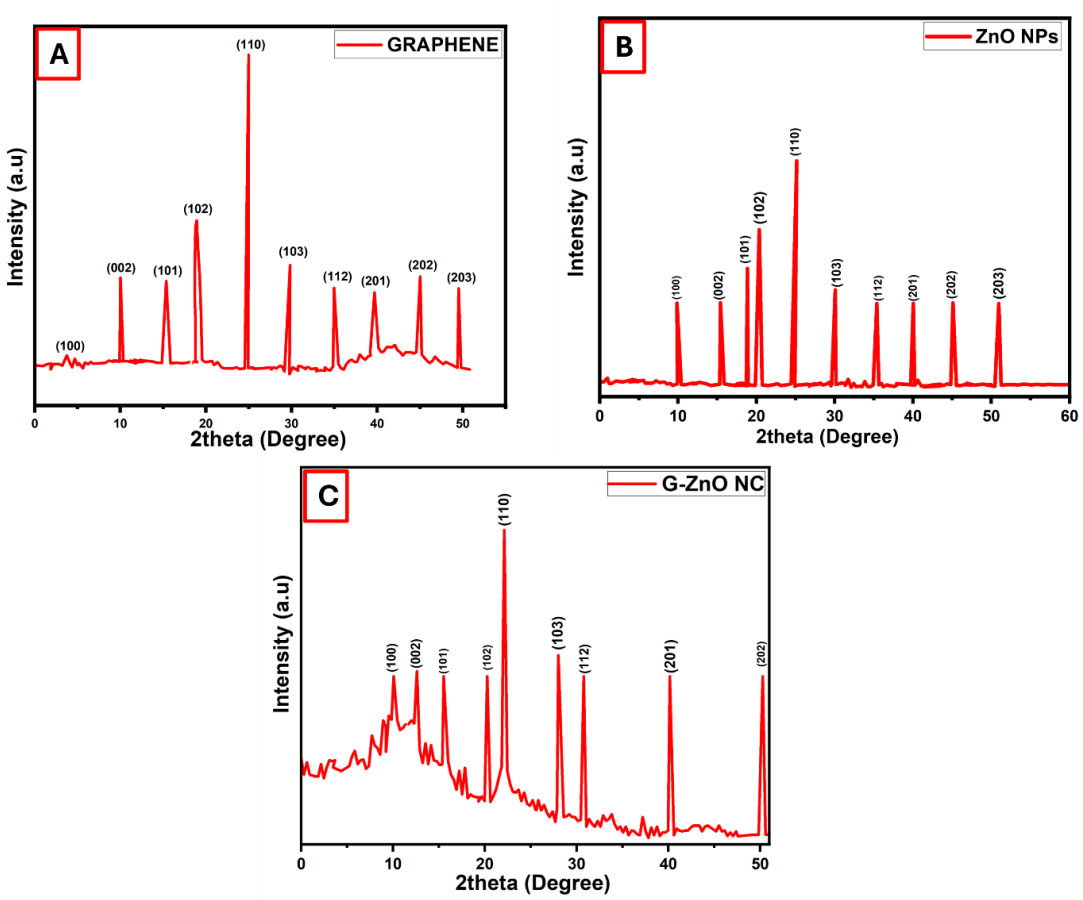

Figure 4: XRD of synthesized (**a**) G (**b**) ZnO NPs and **(c)** G/ZnO NCs

nanoparticl are presented in Figures 4(a), 4(b), and 4(c), respectively. The graphene XRD pattern exhibits a prominent (002) peak at 25.33° and (100) plane: around 42.6°, indicating a layered structure and high crystallinity (Maruthupandy *et al*., 2020). Zinc Oxide nanoparticles, XRD pattern matches the hexagonal phase wurtzite ZnO (JCPDS No. 36-1451), with peaks corresponding to the (100) plane: around 31.7°, (002) plane: around 34.4°, (101) plane: around 36.2°, (102) plane: around 47.5°, (110) plane: around 56.6°, (103) plane: around 62.9°, (112) plane: around 68.0°, (201) plane: around 69.3°, (202) plane: around 76.7°, (203) plane: around 81.3° (Li *et al*., 2012; Abd *et al*., 2019).

The graphene/zinc oxide nanocomposites (G/ZnO NCs), XRD pattern exhibits peaks corresponding to both graphene and ZnO, confirming the successful integration of ZnO nanoparticles into the graphene matrix. The presence of the (002) peak at approximately 26.5° from graphene and the characteristic ZnO peaks indicates that ZnO nanoparticles are coating the graphene surface. The XRD patterns confirm the synthesis of high-quality graphene, ZnO nanoparticles, and G/ZnO nanocomposites (NCs) free from impurities.

Scanning Electron Microscopy (SEM) of the samples.

Scanning Electron Microscopy (SEM) was used to study the surface and morphological characteristics of G, ZnO nanoparticles (NPs), and G/ZnO nanocomposites (NCs). Scanning Electron Microscopy (SEM) of G, ZnO NPs, and G/ZnO NCs are presented in Figures 5(a-b), 5(c-d), and 5(e-f), respectively. The surface morphology of synthesised G, ZnO NPs, and G/ZnO NCs was examined using SEM. The synthesised G exhibited a rough surface, flake-like shape, and non-uniform particle size, with flakes aggregating to form complex structures (Betul *et al*., 2019). Zinc oxide nanoparticles (ZnO NPs) were spherical, densely packed, and had less agglomeration, good connectivity, and homogeneity among particles, with a porous surface attributed to phytochemicals present in the plant extracts used for synthesis (Khors *et al*., 2011; Abd *et al*., 2019)

The graphene/zinc oxide nanocomposites (G/ZnO NCs) displayed a rough, porous structure with aggregated particles, indicating high porosity, and a densely packed arrangement of uniformly distributed spherical particles, suggesting homogeneity in size distribution and structure. The combination of porosity and homogeneous particle distribution highlights the composite's potential for applications that require a high surface area and uniform properties.

Energy Dispersive Spectrum (EDS) of the samples

The elemental composition of the synthesised samples is shown in Figure 6. The EDX result of the synthesised G material shows several elements and their compositions in the obtained G material. In Figure 6(a), there are occurrences of carbon at 63.20 weight % and 65.22 atomic %, oxygen at 20.20 weight % and 22.12 atomic %, aluminium at 6.00 weight % and 2.30 atomic %, iron at 5.30 weight % and 3.04 atomic %, silicon at 3.30 weight % and 4.12 atomic % and potassium at 2.00 weight % and 3.20 atomic %. The result agrees with previous graphene studies (Maruthupandy *et al*., 2020). Graphene, with its high carbon content and excellent electrical conductivity, is a promising material for various applications, including electronics, sensors, and energy storage devices (Nagaraj *et al*., 2020). Figure 6(b) shows the ZnO NPs sample; the EDX spectrum shows a significant presence of zinc (Zn) at 69.40% by weight and oxygen (O) at 22.30%, which aligns with the expected ZnO composition. The minor presence of carbon (C) and silicon (Si) can be attributed to the surface coating and glass used during characterisation.

Figure 6(c) shows the G/ZnO NCs for the composition of both G and ZnO. The EDX spectrum indicates a balanced presence of carbon (C) at 39.00%, zinc (Zn) at 36.36%, and oxygen (O) at 20.24%, with smaller amounts of sulphur and silicon. The presence of carbon and zinc in significant amounts suggests the successful incur-

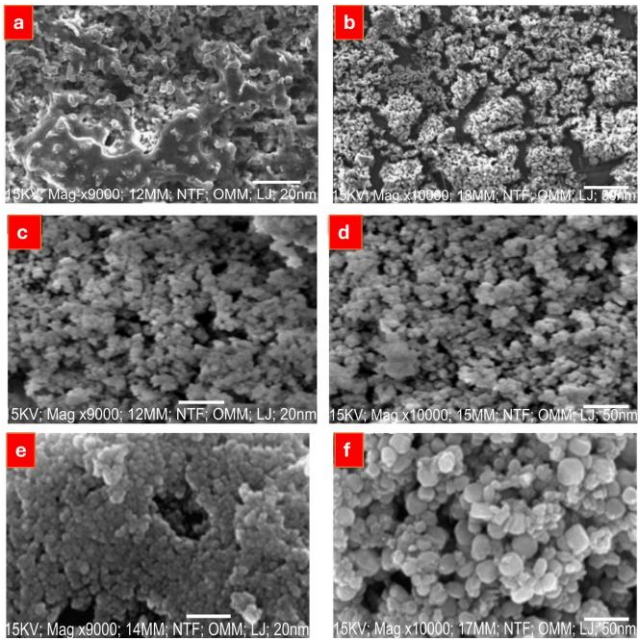

Figure 5: SEM of synthesized **(a-b)** G **(c-d)** ZnO NPs and **(e-f)** G/ZnO NCs

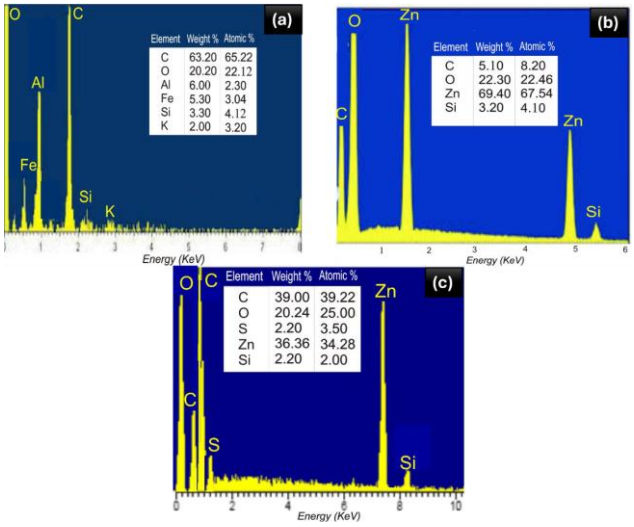

Figure 6: EDX of synthesised **(a)** G **(b)** ZnO NPs and **(c)** G/ZnO NCs

poration of ZnO nanoparticles into the graphene matrix.

Electrical properties of the samples

The electrical behaviour of the samples has been studied, assessed, and plotted in Figure 7. The current-voltage measurement was taken under ambient temperature.

The results, presented in Figure 7 and summarised in Table 2, show that the G/ZnO nanocomposite exhibited improved electrical properties, with a higher current (4.62 μA) and corresponding voltage (0.60 V), compared to graphene (4.22 μA, 0.59 V) and zinc oxide nanoparticles (2.51 μA, 0.51 V). The synergistic combination of graphene and zinc oxide nanoparticles enhanced electrical conductivity, forming a percolative network that facilitated efficient electron transport and interconnectivity between particles, aligning with percolation theory

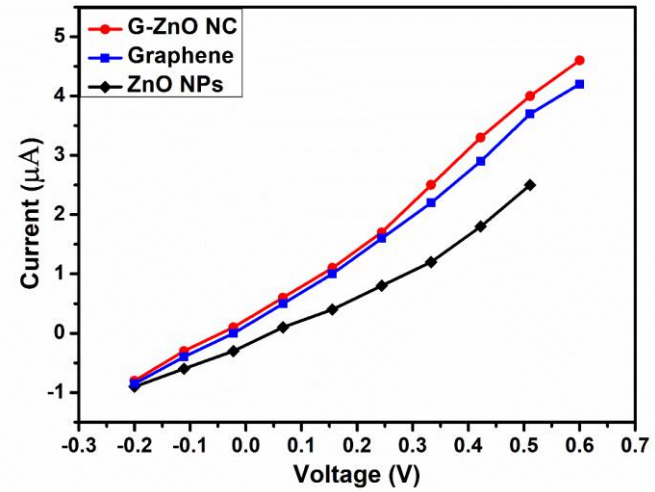

Figure 7: Graphs of current versus voltage for G, ZnO NPs, and G/ZnO NCs thin films

Conclusion

The green synthesis and characterisation of graphene (G), zinc oxide nanoparticles (ZnO NPs), and graphene/zinc oxide nanocomposite (G/ZnO NCs) have been established, which have the potential for use in optoelectronic applications. The UV-Vis absorption spectra of G, ZnO NPs, and G/ZnO NCs were analysed. Graphene exhibited absorption edges at 330 nm and 340 nm, while ZnO NPs displayed a sharp absorption edge at 295 nm, and G/ZnO NCs showed a broad absorption spectrum with increased absorbance around 300-400 nm. This indicates strong absorption due to G/ZnO interactions, modifying the optical properties of ZnO. The FTIR spectra revealed distinct absorption peaks corresponding to functional groups in G, ZnO NPs, and G/ZnO NCs.

Table 2: The electrical characteristics of G, ZnO NPs, and G-ZnO NCs

Parameter	G	ZnO NPs	G/ZnO NCs
Length Between Probes (cm)	1.9	1.9	1.9
Area of Thin Film (cm^2)	5.94	5.94	5.94
Current, I (μA)	4.22	2.51	4.62
Voltage, V (V)	0.59	0.51	0.60
Resistance, R (k Ω)	139.81	203.19	129.87
Resistivity, ρ (Ω-m)	437.32	634.38	405.56
Sheet Resistance (ohms)	1987.82	2883.55	1843.45
Conductivity, σ (S/m)	2.29×10^{-3}	1.58×10^{-3}	2.46×10^{-3}

The graphene/zinc oxide nanocomposites (G/ZnO NCs) spectrum showed significant peaks indicating O-Zn-O bending vibrations, C-H bending vibrations, and C=C stretching vibrations. The FTIR analysis provided insights into the surface chemistry, bonding characteristics, and properties of the composite material. The XRD of Graphene exhibited a prominent (002) peak at 25.33°, indicating high crystallinity. Zinc oxide nanoparticles (ZnO NPs) matched the hexagonal phase wurtzite ZnO with characteristic peaks. The graphene/zinc oxide nanocomposites (G/ZnO NCs) XRD pattern confirmed the successful integration of ZnO NPs into the graphene matrix.SEM reveals that the Graphene exhibited a rough, flake-like surface, while ZnO NPs were spherical and densely packed. The G/ZnO NCs displayed a rough, porous structure with aggregated particles, indicating high porosity. The composite's homogeneous particle distribution and porosity suggest potential for applications requiring a high surface area. The electrical conductivity evaluated showed improvement in the properties of ZnO NPs due to synthesis with *Phyllanthus Amarus extract*. The synthesised G/ZnO NCs have the potential to enhance optoelectronic device performance because of the injection of excited electrons into the conduction band due to a reduction in electron recombination. These findings demonstrate the potential of graphene/zinc oxide nanocomposite as an electron transport layer for solar cells and other optoelectronics applications. Production of nanoparticles with plant extract at a low cost is viable and possible. Further work on the application of this research work on active solar cells and other optoelectronic devices should be a subject of future research to ascertain its viability and efficiency.

Reference

Abd, E., Alrubaie, A.-A. & Kadhim, R. E. (2019). *Synthesis of ZnO Nanoparticles from Olive Plant Extract* (Vol. 19, Issue 2).

Alamu, G. A., Adedokun, O., Bello, I. T. & Sanusi, Y. K. (2021). Plasmonic enhancement of visible light absorption in Ag-TiO_2 based dye-sensitized solar cells. *Chemical Physics Impact*, *3*, 100037.

https://doi.org/10.1016/j.chphi.2021.100037

Arefi, M. R. & Rezaei-Zarchi, S. (2012). Synthesis of Zinc Oxide Nanoparticles and Their Effect on the Compressive Strength and Setting Time of Self-Compacted Concrete Paste as Cementitious Composites. *International Journal of Molecular Sciences*, *13*(4), 4340–4350. https://doi.org/10.3390/ijms13044340

Boutilier, M. S. H., Sun, C., O'Hern, S. C. & Au, H., Hadjiconstantinou, N. G., and Karnik, R. (2014). Implications of Permeation through Intrinsic Defects in Graphene on the Design of Defect-Tolerant Membranes for Gas Separation. *ACS Nano*, *8*(1), 841–849. https://doi.org/10.1021/nn405537u

Chakraborty, A., Lucarelli, G., Xu, J., Skafi, Z., Castro-Hermosa, S., Kaveramma, A. B., Balakrishna, R. G. & Brown, T. M. (2024). Photovoltaics for indoor energy harvesting. *Nano Energy*, *128*, 109932. https://doi.org/10.1016/j.nanoen.2024.109932

Djuriić, A. B., Ng, A. M. C. & Chen, X. Y. (2010). ZnO nanostructures for optoelectronics: Material properties and device applications. *Progress in Quantum Electronics*, *34*(4), 191–259. https://doi.org/10.1016/j.pquantelec.2010.04.001

Farghali, M., Osman, A. I., Chen, Z., Abdelhaleem, A., Ihara, I., Mohamed, I. M. A., Yap, P.-S. & Rooney, D. W. (2023). Social, environmental, and economic consequences of integrating renewable energies in the electricity sector: a review. *Environmental Chemistry Letters*, *21*(3), 1381–1418. https://doi.org/10.1007/s10311-023-01587-1

Gupta, Chatterjee, S., Ray, A. K. & Chakraborty, A. K. (2015). Graphene–metal oxide nanohybrids for toxic gas sensor: A review. *Sensors and Actuators B: Chemical*, *221*, 1170–1181. https://doi.org/10.1016/j.snb.2015.07.070

Hao, Q., Li, P., Liu, J., Huang, J. & Zhang, W. (2023). Bandgap engineering of high mobility two-dimensional semiconductors toward optoelectronic devices. *Journal of Materiomics*, *9*(3), 527–540. https://doi.org/10.1016/j.jmat.2022.11.009

Hoseinpour, V. , Souri, M. , Ghaemi, N. & Shakeri, A. (2017). Optimization of green synthesis of ZnO nanoparticles by Dittrichia graveolens (L.) aqueous extract. *Health Biotechnol. Biopharma,* 39–49.

Huang, D., Yang, T., Mo, Z., Guo, Q., Quan, S., Luo, C. & Liu, L. (2016). Preparation of Graphene/TiO_2 Composite Nanomaterials and Its Photocatalytic Performance for the Degradation of 2,4-Dichlorophenoxyacetic Acid. *Journal of Nanomaterials*, *2016*, 1–11. https://doi.org/10.1155/2016/5858906

Jayarambabu, N., Siva Kumari, B., Venkateswara Rao K. & Prabhu Y.T. (2014). Germination and Growth Characteristics of Mungbean Seeds (Vigna radiata L.) affected by Synthesized Zinc Oxide Nanoparticles. *International Journal of Current Engineering and Technology*.

Kachere, A. R., Kakade, P. M., Kanwade, A. R., Dani, P., Mandlik, N. T., Rondiya, S. R., Dzade, N. Y., Jadkar, S. R. & Bhosale, S. V. (2021). Zinc Oxide/Graphene Oxide Nanocomposites: Synthesis, Characterization and Their Optical Properties. *ES Materials and Manufacturing*. https://doi.org/10.30919/esmm5f516

Khalil, M., Ismael, E., Mohamed, H. & Elaasser, M. (2020). Green synthesis of zinc oxide nanoparticles using Portulaca oleracea (Regla seeds) extract and its biomedical applications. *Egyptian Journal of Chemistry*, *0*(0), 0–0. https://doi.org/10.21608/ejchem.2020.45592.2930

Kumar, N., Salehiyan, R., Chauke, V., Joseph Botlhoko, O., Setshedi, K., Scriba, M., Masukume, M. & Sinha Ray, S. (2021). Top-down synthesis of graphene: A comprehensive review. In *FlatChem* (Vol. 27). Elsevier B.V. https://doi.org/10.1016/j.flatc.2021.100224

Li, B., Liu, T., Wang, Y. & Wang, Z. (2012). ZnO/graphene-oxide nanocomposite with remarkably enhanced visible-light-driven

photocatalytic performance. *Journal of Colloid and Interface Science*, *377*(1), 114–121. https://doi.org/10.1016/j.jcis.2012.03.060

Liu, X., Liu, W., Ko, M., Park, M., Kim, M. G., Oh, P., Chae, S., Park, S., Casimir, A., Wu, G. & Cho, J. (2015). Metal (Ni, Co)-Metal Oxides/Graphene Nanocomposites as Multifunctional Electrocatalysts. *Advanced Functional Materials*, *25*(36), 5799–5808. https://doi.org/10.1002/adfm.201502217

Maalouf, A., Okoroafor, T., Jehl, Z., Babu, V. & Resalati, S. (2023). A comprehensive review on life cycle assessment of commercial and emerging thin-film solar cell systems. *Renewable and Sustainable Energy Reviews*, *186*, 113652. https://doi.org/10.1016/j.rser.2023.113652

Machín, A. & Márquez, F. (2024). Advancements in Photovoltaic Cell Materials: Silicon, Organic, and Perovskite Solar Cells. *Materials*, *17*(5), 1165. https://doi.org/10.3390/ma17051165

Malhotra, S. P. K. & Alghuthaymi, M. A. (2022). Biomolecule-assisted biogenic synthesis of metallic nanoparticles. In *Agri-Waste and Microbes for Production of Sustainable Nanomaterials* (pp. 139–163). Elsevier. https://doi.org/10.1016/B9780-12-823575-1.00011-1

Maruthupandy, M., Qin, P., Muneeswaran, T., Rajivgandhi, G., Quero, F. & Song, J.-M. (2020). Graphene-zinc oxide nanocomposites (G-ZnO NCs): Synthesis, characterization and their photocatalytic degradation of dye molecules. *Materials Science and Engineering: B*, *254*, 114516. https://doi.org/10.1016/j.mseb.2020.114516

Nagaraj, E., Shanmugam, P., Karuppannan, K., Chinnasamy, T. & Venugopal, S. (2020). The biosynthesis of a graphene oxide-based zinc oxide nanocomposite using *Dalbergia latifolia* leaf extract and its biological applications. *New Journal of Chemistry*, *44*(5), 2166–2179. https://doi.org/10.1039/C9NJ04961D

O'Hern, S. C., Boutilier, M. S. H., Idrobo, J.-C., Song, Y., Kong, J., Laoui, T., Atieh, M. & Karik, R. (2014). Selective Ionic Transport through Tunable Subnanometer Pores in Single-Layer Graphene Membranes. *Nano Letters*, *14*(3), 1234–1241. https://doi.org/10.1021/nl404118f

Payrazm, S., Baghshahi, S., Sadeghian, Z. & Aliabadizadeh, A. (2022). Structural and Optical Characterization of ZnO-Graphene Nanocomposite Quantum Dots. *Iranian Journal of Materials Science and Engineering*, *19*(3). https://doi.org/10.22068/ijmse.2603

Qu, J., Luo, C., Zhang, Q., Cong, Q. & Yuan, X. (2013). Easy synthesis of graphene sheets from alfalfa plants by treatment of nitric acid. *Materials Science and Engineering: B*, *178*(6), 380–382. https://doi.org/10.1016/j.mseb.2013.01.016

Rahman, F., Majed Patwary, M. A., Bakar Siddique, Md. A., Bashar, M. S., Haque, Md. A., Akter, B., Rashid, R., Haque, Md. A. & Royhan Uddin, A. K. M. (2022). Green synthesis of zinc oxide nanoparticles using *Cocos nucifera* leaf extract: characterization, antimicrobial, antioxidant and photocatalytic activity. *Royal Society Open Science*, *9*(11). https://doi.org/10.1098/rsos.220858

Shahryari, Z., Yeganeh, M., Gheisari, K. & Ramezanzadeh, B. (2021). A brief review of the graphene oxide-based polymer nanocomposite coatings: preparation, characterization, and properties. *Journal of Coatings Technology and Research*, *18*(4), 945–969. https://doi.org/10.1007/s11998-021-00488-8

Sin Tee, T., Chun Hui, T., Wu Yi, C., Chi Chin, Y., Umar, A. A., Riski Titian, G., Hock Beng, L., Kok Sing, L., Yahaya, M. & Salleh, M. M. (2016). Microwave-assisted hydrolysis preparation of highly crystalline ZnO nanorod array for room temperature photoluminescence-based CO gas sensor. *Sensors and Actuators B: Chemical*,

227, 304–312. https://doi.org/10.1016/j.snb.2015.12.058

Sun, K., Xiao, H., Liu, S., You, S., Yang, F., Dong, Y., Wang, W. & Liu, Y. (2020). A Review of Clean Electricity Policies—From Countries to Utilities. *Sustainability*, *12*(19), 7946. https://doi.org/10.3390/su12197946

Verduci, R., Romano, V., Brunetti, G., Yaghoobi Nia, N., Di Carlo, A., D'Angelo, G. & Ciminelli, C. (2022). Solar Energy in Space Applications: Review and Technology Perspectives. *Advanced Energy Materials*, *12*(29). https://doi.org/10.1002/aenm.202200125

Wu, W., Wen, X. & Wang, Z. L. (2013). Taxel-Addressable Matrix of Vertical-Nanowire Piezotronic Transistors for Active and Adaptive Tactile Imaging. *Science*, *340*(6135), 952–957. https://doi.org/10.1126/science.1234855